Vibrational Overtone Spectroscopy and Overtone Intensities of Cyclohexadiene Iron Tricarbonyl and 1,3-Cyclohexadiene

A. V. Fedorov* and D. L. Snavely

Department of Chemistry and Center for Photochemical Sciences, Bowling Green State University, Bowling Green, Ohio 43403

H. G. Kjaergaard

Department of Chemistry, University of Otago, Post Office Box 56, Dunedin, New Zealand

K. M. Gough and B. Billinghurst

Department of Chemistry, University of Manitoba, Winnipeg, Manitoba R2T 2N2, Canada

Received: June 5, 2000; In Final Form: September 8, 2000

The CH stretching overtone spectra of liquid cyclohexadiene iron tricarbonyl (CHDIT) have been recorded for the first, second, and third overtone regions ($\Delta v = 2-4$). The gaseous spectrum of CHDIT has also been obtained for the first overtone region ($\Delta v = 2$). Observed transitions are assigned to the overtones of different nonequivalent CH bonds and to the local mode−normal mode combination bands. Oscillator strengths have been calculated with the harmonically coupled anharmonic oscillator (HCAO) local mode model and ab initio dipole moment functions. The theoretical values have been compared to the experimental oscillator strengths and agree well with experiment. The comparison of the overtone spectrum of CHDIT to the corresponding spectrum of uncomplexed 1,3-cyclohexadiene reveal changes that occur in the ligand upon complexation with iron tricarbonyl. The presence of the metal lengthens the terminal olefinic CH bond by 0.002 Å and shortens the nonterminal olefinic CH by 0.001 Å. The axial and equatorial CH bonds of the free ligand become similar in length in the complex. The implications of the observed spectral features to the structure and bonding in the complex are discussed.

Introduction

Transition metal complexes are used as catalysts in many chemical processes.[1] The basis of this catalytic activity is the ability of the unoccupied metal d-orbitals to share the electrons with lone pairs or π or aromatic clouds of the ligands and form fairly strong bonds. The formation of these bonds significantly alters the electronic structure and properties of the ligands. π-Bonded transition metal complexes of olefins can serve as examples of such compounds. The formation of the metal−olefin bond makes olefinic π-systems more susceptible to the various types of chemical interactions resulting in π-system rearrangements[2] or hydrogen shifts.[3] Transition metal complexes can be considered as intermediates of the catalytic process. The structure and properties of metal carbonyl complexes of olefins have been studied by many techniques including NMR,[4−6] X-ray diffraction,[7] and microwave spectroscopy.[8]

Vibrational overtone spectroscopy provides an alternative for elucidating the influence of metal bonding on the structure and properties of olefins. It probes molecules at high internal energies with vibrational energy localized in the XH bond stretch (X = C, N, O). The experimentally observed transitions are well described by the local mode (LM) model.[9] The relative energies of overtone peaks provide information about relative lengths of different XH bonds. Within one overtone level, the higher the energy of transition, the shorter the bond. This relationship, in conjunction with results of reasonably high-level ab initio calculations, presents a powerful tool for examining the structure and conformations of these molecules. The approximately linear relationship between the ab initio XH bond lengths and overtone transition wavenumbers has been well established for overtone transitions of halogenated aromatic molecules,[10,11] alkanes,[12,13] olefins,[14] and alcohols and amines.[15]

The direct comparison of the overtone spectrum of an organometallic complex with that of the corresponding free ligand provides information about the CH bond length changes that occur upon complexation. On the basis of the experimental results, the change in the π-bond strength can also be estimated. Moreover, the appearance of additional bands that were absent in the ligand spectrum and changes in the relative intensities of the free ligand transitions are indicative of changes in vibrational coupling initiated by the metal bonding.

Vibrational overtone spectroscopy has previously been used to study changes induced by the metal bonding in ferrocene and related compounds,[16,17] butadiene iron tricarbonyl,[18] and chromium tricarbonyls of benzene and cycloheptatriene.[19] With the exception of ferrocene and its related compounds,[17] only the third overtone spectra have been recorded and analyzed for these complexes. The present study is a continuation of this previous work with a focus on cyclohexadiene iron tricarbonyl (CHDIT, **1**). A wider energy range involving several overtones has been studied and the experimental results have been compared to calculations of both transition energies and overtone intensities. The recent work on the overtones of gaseous 1,3-cyclohexadiene[20] (1,3-CHD, **2**) has been used for comparison.

10.1021/jp0020337 CCC: $20.00
Published on Web 03/08/2001

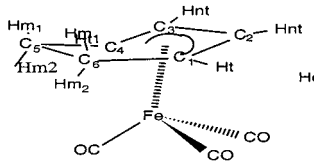

1

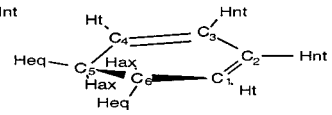

2

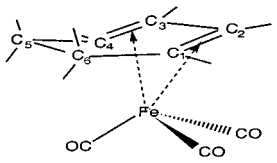

3

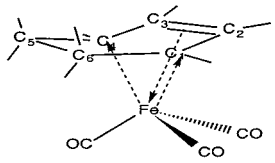

4

Bonding in CHDIT has been the subject of several theoretical and experimental studies.[4,7,8,21] Hückel molecular orbital interaction calculations[21] indicate that nearly degenerate $2e_s$ and $2e_a$ orbitals of the $Fe(CO)_3$ fragment strongly interact with both highest bonding (π_2) and lowest antibonding (π_3) orbitals of 1,3-diene fragment. This would lead to two possible structures **3** and **4** shown above. Low-temperature ^{13}C NMR experiments[4] have been devoted to determining which of the two alternative structures better represents the bonding in CHDIT in solution. The barrier for rearrangement between **3** and **4** was estimated to be 8.8 kcal/mol[4] but these studies did not clarify the structure of the complex.

Limited information exists in the literature concerning the infrared spectroscopy of CHDIT in the CH stretch fundamental region. Burton et al.[22] reported six bands in this region for the neat liquid CHDIT. To our knowledge, no normal-mode analysis has been done for CHDIT.

Microwave spectroscopic studies revealed the basic "piano stool" type structure for CHDIT[8] in agreement with X-ray diffraction data.[7] The microwave-determined CC bonds are different for the ligand[23] and the complex.[8] The central diene bond shortened upon complexation by 0.072 Å (1.470 Å in CHD; 1.398 Å in CHDIT) but did not reach the length of the double bonds in the free ligand (1.340 Å). These double bonds become longer (1.416 Å) in the complex. All of these results indicate that the structure found by microwave spectroscopy lies somewhere between the two extremes **3** and **4**. The CC bond lengths obtained from X-ray diffraction[7] are in agreement with the microwave spectroscopy findings.

While the CH bond lengths could not be determined by X-ray diffraction, the microwave spectral data[23] for CHDIT showed only two types of CH bond: olefinic (1.080 Å) and methylenic (1.099 Å). In that paper, the CH bond lengths were assigned values calculated for pentadiene, with an assumption of standard sp^2 and sp^3 bond angles. The authors noted that the final results were fairly insensitive to changes of 0.01 Å in these values. In a similar manner, the microwave data for the free ligand, 1,3-CHD, also showed only two types of CH bond, and again these were the olefinic (1.086 Å) and methylenic (1.100 Å). However, the overtone spectra[20] of 1,3-CHD show irrefutable evidence for the existence of two types of methylenic CH (axial and equatorial). These overtone results are corroborated by high-level ab initio calculations.[20]

Vibrational overtone spectroscopy[9] provides specific information about the number of different CH bonds, their relative lengths, and thus the changes in length that occur upon complexation. Direct information about CC bonds is not possible with overtone spectroscopy, while the precision of CH bond measurements with microwave spectroscopy is less than that possible with CH overtones. Therefore, a deeper understanding of the nature of the bonding in the complexed ligand is best achieved through deductions based on CC bond length information from microwave spectroscopy and CH bond length information from CH overtone spectroscopy.

Experimental Section

1,3-CHD (97% purity) was obtained from Aldrich, and CHDIT (97% purity) was purchased from Strem Chemicals. Both compounds have been used without further purification. Because of the moderate air sensitivity of the organometallic complex, all transfers and solution preparations have been conducted under an inert atmosphere of nitrogen or argon by standard techniques. The solvents were degassed prior to use by passing nitrogen through the solvent for at least 2 h.

All CCl_4 solution spectra and second and third overtone liquid spectra have been recorded on a Mattson Galaxy series FTIR spectrometer with a 1 cm quartz cuvette and 2 cm^{-1} resolution. At least 1000 scans were averaged for each spectrum. A Pb/Se detector has been used in the 4000−10 000 cm^{-1} region (first and second overtones), and a Si detector has been used to record the spectra above 10 000 cm^{-1} (third overtone). Neat liquid spectra have been obtained for the second and third overtones for both CHD and CHDIT. Because of the saturation of the neat liquid spectra in the first overtone region, the first and second overtones of both ligand and complex have also been recorded for 0.6 M carbon tetrachloride solutions. The second overtone spectra recorded in CCl_4 solution were very similar to those from the neat liquid samples for both CHD and CHDIT. This indicates the absence of CHDIT−solvent interactions, which were observed for chromocene and manganocene[24] in CCl_4, and allows one to compare solution spectra to the neat liquid results.

The first overtone spectra for both liquid and gaseous CHDIT have been obtained with a Wilmad Glass variable path length cell (3 m path length) and a Bio-Rad FTS-40 spectrometer. The sample was introduced into the cell via a sidearm that could be opened to the cell when the temperature was appropriate (∼120 °C at the bottom of the sidearm; ∼100 °C at the bottom of the cell). The elevated temperature was achieved by wrapping the cell and sidearm in heating tape and covering the entire apparatus in fiberglass insulation. When the cell had reached the desired temperature, the background spectrum was acquired. The sidearm was opened to allow the CHDIT vapor to enter the cell. A total of 128 scans were recorded and coadded to obtain the spectrum. To obtain the liquid-phase spectrum, the bottom of the multipass cell was allowed to cool so that the CHDIT condensed onto the windows, forming a uniform liquid layer (thickness about 0.5 mm). Under these experimental conditions, the CHDIT vapor pressure above the liquid layer was not high enough to contaminate the liquid-phase spectrum with gas-phase absorptions. Again, 128 scans were measured and coadded to obtain the spectrum.

The experimental spectra have been deconvoluted with Mattson PeakSolve and Bomem-Grams deconvolution software. Peak positions were determined from the deconvoluted spectra. The experimental relative intensities were obtained by comparing the areas under the peaks produced by the curve-fitting procedure. The experimental oscillator strengths, *f*, have been calculated from the areas under the deconvoluted peaks by use of eq 1 for the gas-phase spectra and eq 2 for the liquid-phase data:[25,26]

$$f_{e\leftarrow g} = (8.026 \times 10^{-7}\ \text{Torr·m·cm})\frac{1}{pl}\int A(\tilde{\nu})\,d\tilde{\nu} \quad (1)$$

$$f_{e\leftarrow g} = (4.335 \times 10^{-11}\ \text{mol·l}^{-1}\text{·m·cm})\frac{9n}{(n^2+2)^2}\frac{1}{Ml}\int A(\tilde{\nu})\,d\tilde{\nu} \quad (2)$$

where p is the gaseous sample pressure in the cell in Torr, n is the refractive index of a liquid sample ($n = 1.47$ for 1,3-CHD and $n = 1.62$ for CHDIT), M is the molar concentration of the sample, l is the path length, and A is absorbance. The molar concentrations of the neat liquid samples, calculated from the densities, have been determined to be 10.5 M for 1,3-CHD and 6.3 M for CHDIT. The vapor pressure of gaseous CHDIT in the cell was estimated to be about 0.5 Torr.

Calculation of Overtone Intensities and Molecular Geometries. The CH stretching spectra have been analyzed within the harmonically coupled anharmonic oscillator (HCAO) local mode model. The dipole moment functions and local mode parameters were calculated at the Hartree−Fock (HF) self-consistent field level of theory with a 6-311+G(d,p) basis set. Dipole moment functions have been generated as a series expansion in the two CH stretching coordinates for the aliphatic CH_2 and a single CH coordinate for the olefinic CH bonds. Fully optimized geometries have been calculated at the HF level of theory and with density functional theory.

The oscillator strength of a vibrational transition from the vibrational ground state, g, to the vibrationally excited state, e, is given by[25,27]

$$f_{eg} = (4.702\ \text{cm·D}^{-2})\tilde{\nu}_{eg}|\vec{\mu}_{eg}|^2 \quad (3)$$

where $\tilde{\nu}_{eg}$ is the vibrational wavenumber of the transition and $|\vec{\mu}_{eg}|^2$ is the transition dipole moment matrix element in debyes.

The harmonically coupled anharmonic oscillator (HCAO) local mode model[27−31] has been used to describe the CH stretching vibrational modes of the molecules. The coupling between CH bonds is significant only when the hydrogen atoms are attached to the same carbon atom[30] and only coupling between the two CH bonds in the aliphatic groups was included. Within this approximation, the 1,3-CHD and CHDIT are described by a single CH oscillator for the olefinic CH bonds and an asymmetric CH_2 group for the aliphatic CH bonds similar to the CH_2 group in cyclohexane. The HCAO local mode models for an asymmetric CH_2 group and a single CH bond have been described in detail elsewhere,[26−30] and only a brief outline is given here. The eigenstates are labeled $|v_1\rangle_{nt}$ and $|v_2\rangle_t$ or $|v_1\rangle_{ol}$ and $|v_2\rangle_{ol'}$ for the nonterminal and terminal olefinic CH bonds, respectively, and $|v_1\rangle_{m1}|v_2\rangle_{m2}$ or $|v_1\rangle_{ax}|v_2\rangle_{eq}$ for the CH bonds in asymmetric CH_2 groups.

For a single CH bond, the Hamiltonian is simply that of a Morse oscillator:

$$\frac{\hat{H} - E_{|0\rangle}}{hc} = v_i\tilde{\omega}_i - (v_i^2 + v_i)\tilde{\omega}_i x_i \quad (4)$$

where $\tilde{\omega}_i$ and $\tilde{\omega}_i x_i$ are the local mode frequency and anharmonicity, respectively, and $E_{|0\rangle}$ is the energy of the vibrational ground state. The CH_2 groups are treated in a similar manner, with Morse oscillators describing the diagonal Hamiltonian and the off-diagonal terms given by harmonic coupling terms. The equations for the asymmetric CH_2 are identical to the equations used for cyclohexane.[29] The effective coupling parameter, γ', which contains both kinetic and potential energy coupling, is estimated from ab initio calculations of the force constants and the optimized geometry. The effective coupling between CH stretching oscillators and the mixed dipole moment function terms mainly affect the local mode combination states, which typically appear only in the lower overtones. The magnitude of this coupling is not very sensitive to the absolute value of γ'. With the HF/6-311+G(d,p) method, the values of $\gamma' = 15.1$ and 7.3 cm^{-1} have been obtained for 1,3-CHD and CHDIT, respectively.

The dipole moment function is expressed as a series expansion in the internal CH displacement coordinates, q. For an isolated CH stretching oscillator the following expression is used:[26]

$$\vec{\mu} = \sum_i \vec{\mu}_i q^i \quad (5)$$

where $\vec{\mu}_i$ is $1/i!$ times the ith order derivative of the dipole moment function with respect to q. To determine the expansion coefficients, $\vec{\mu}_i$, ab initio molecular orbital theory is used to calculate the dipole moment as a function of q. A one-dimensional grid consisting of nine points around the equilibrium geometry, with a step size of 0.05 Å, i.e., a maximum displacement of ±0.2 Å, is calculated. In eq 5, we have taken the expansion to sixth order, instead of fourth order as was done previously, to improve the results for the local mode parameters.

For the CH_2 group, the expansion is two-dimensional and a two-dimensional grid in the two internal displacement coordinates is calculated to provide the mixed terms in the expansion of the dipole moment function.[29] Only the second- and third-order mixed terms are included in the calculation. The mixed terms are important primarily for the local mode combination states in the lower overtones and have been determined from a 5×5 grid for CHDIT.

The geometry of 1,3-CHD and CHDIT was calculated at the HF/3-21G(*) and HF/6-311+G(d,p) level. The effect of electron correlation on geometry of the complex and uncomplexed ligand was investigated by density functional theory with the perturbative Becke−Perdew method with full polarization basis set (pBP/DN** as defined within Spartan[32]). For the dipole moment function calculation, the optimized geometry and the dipole moment at displaced geometries were all calculated with Gaussian94[33] at the HF level of theory with the 6-311+G(d,p) basis sets as defined within Gaussian94. Previous calculations have shown that the HF/6-31G(d) basis set gives good relative intensities within a given overtone, whereas larger basis sets are required to improve on the absolute overtone intensities.[26,34] Electron correlation in the calculation of the dipole moment function seems to have little effect on CH stretching overtone intensities and was not used here to calculate intensities.[35−37]

The local mode parameters for an isolated CH stretching mode can be calculated from ab initio calculations of the force constant and the derivative of the force constant along the internal CH stretching coordinate.[38] The force constants are obtained from the molecular energies calculated in the one-dimensional grids already calculated for the dipole moment functions. The ab initio local mode determined parameters $\tilde{\omega}_i$ and $\tilde{\omega}_i x_i$ have to be scaled in a manner similar to the scaling commonly done with calculated IR frequencies. The scaling factors for olefinic and aliphatic CH bonds were determined as the average of the ratios of calculated to experimental frequencies and anharmonicities for the appropriate CH bonds in cyclohexane,[29,41] naphthalene,[39] and benzene.[40] The scaling factors obtained with the HF/6-311+G(d,p) method and a nine-point 0.05 Å spacing grid are given in Table 1. The errors in

TABLE 1: Scaling Factors for the HF/6-311+G(d,p) Method

	vapor[a]	liquid[b]
$\tilde{\omega}_{ol}$	0.9488	0.9447
$\tilde{\omega}_{al}$	0.9523	0.9449
$\tilde{\omega}x_{ol}$	0.941	0.926
$\tilde{\omega}x_{al}$	0.959	0.942

[a] Estimated with use of naphthalene (ref 39) and cyclohexane (ref 29) experimental values. [b] Estimated with use of benzene (ref 40) and cyclohexane (ref 41) experimental values.

the calculated $\tilde{\omega}_i$ and $\tilde{\omega}_i x_i$ were estimated to be on the order of 10 and 1 cm^{-1}, respectively. Overall, the scaled ab initio local mode parameters (Tables 2 and 3) should provide a good estimate of $\tilde{\omega}_i$ and $\tilde{\omega}_i x_i$.

Results and Discussion

The CH stretching overtone spectra for $\Delta v = 2$ of CHDIT and 1,3-CHD CCl_4 solutions are presented in Figure 1. The spectra for $\Delta v = 3-4$ of liquid CHDIT and 1,3-CHD are given in Figures 2 and 3, and the spectra for $\Delta v = 2$ of gas-phase CHDIT and 1,3-CHD are given in Figure 4. Experimentally observed and calculated LM parameters for CH bonds of the ligand and the complex are tabulated in Tables 2 and 3. The observed and calculated peak energies, relative intensities, and assignments are given in Table 4 for 1,3-CHD and in Tables 5 and 6 for CHDIT. Results of geometry optimizations for 1,3-CHD and CHDIT at different levels of theory are presented in Table 7. The relative CH olefinic to CH methylenic intensities are displayed in Table 8. The total absolute oscillator strengths for all examined overtones are shown in Table 9.

The experimental uncertainties in determining the LM parameters are particularly high for CH_{eq} of CHD and CH_{ol_t} of CHDIT. This is because these two bands are located in the most congested regions of the spectrum and overlap with other transitions. This situation makes the deconvolution rather difficult and leads to the larger uncertainty in determining the transition energy. This, in turn, causes the larger uncertainties for the LM parameters.

A. Experimental and Ab Initio LM Parameters. Both experimental and calculated parameters in Tables 2 and 3 show an expected trend: the olefinic CHs possess higher mechanical frequencies and lower anharmonicities compared to the aliphatic CHs. The agreement between the calculated and experimental liquid-phase values is very good for CH olefinic bonds of 1,3-CHD and is similar to the gas-phase results.[20] For the aliphatic CHs of 1,3-CHD, the difference between the calculated and experimental parameters increases, especially for the anharmonicities, but the agreement still remains good, reproducing the correct trend. The agreement is poorer for CHDIT, where calculated numbers reproduce the experimental trends correctly but do not correspond closely to the experimental LM parameters. This could be due to the limited experimental values and larger uncertainties in determining the LM parameters for liquid CHDIT and due to uncertainty in using scaling factors for the complexes. The overall agreement, however, is still reasonable since calculated LM parameters scaled for the liquid phase yield transition energies close to the experimental peak positions for both the ligand and the complex. The experimental LM parameters were used in Tables 4 and 5.

B. Band Assignments and Intensities. The liquid phase overtone spectrum of 1,3-CHD closely resembles previously recorded gas-phase data.[20] All corresponding transitions are red-shifted by 10−55 cm^{-1}, consistent with the general trend observed for the liquid versus gas-phase spectra. The spectral assignments for the liquid-phase transitions displayed in Table 4 are similar to those obtained for the gaseous 1,3-CHD.[20] The agreement between calculated and experimental wavenumbers and absolute intensities is good. Significant differences in the absolute oscillator strengths are observed between neat liquid and the CCl_4 solution intensities for the states in the $\Delta v = 3$ region. These differences are due to the significant overlap of these states with the intense pure LM transitions and broad line widths in the liquid phase. The deconvolution of the closely lying peaks entails large uncertainties.

Comparison between the spectra of 1,3-CHD and CHDIT from Figures 1−3 reveals dramatic changes, which the complexation with the metal tricarbonyl introduces to the ligand. The olefinic band of 1,3-CHD appears to be split into two ($\Delta v = 2$) or three ($\Delta v = 3, 4$) components in the CHDIT spectrum. In addition, two partially overlapped transitions appear in the region where CH aliphatic bonds are expected to absorb for CHDIT, in contrast to the two distinct CH axial and equatorial bands of uncomplexed 1,3-CHD separated by hundreds of wavenumbers. These experimental data indicate that the CH olefinic bonds in 1,3-CHD become different upon complexation and the axial and equatorial CH bonds become similar in length. This is consistent with the results of the geometry optimization calculations for all levels of theory shown in Table 7. At the HF/6-311+G(d,p) level, for instance, the 0.005 Å difference between CH_{ax} and CH_{eq} bonds of 1,3-CHD becomes only 0.002 Å in the complex. On the other hand, the CH_{ol} bonds, which are similar in length in the uncomplexed ligand, become 0.005 Å different in CHDIT. The DFT pBP/DN** geometries show the same ordering of bonds and trends upon complexation. However, longer CH bond lengths and larger differences in the CH aliphatic bond lengths compared to the Hartree−Fock results are predicted.

The correlation between the optimized ab initio bond lengths and the overtone band maximum position is well established.[10−15] On the basis of the calculated CH bond lengths in the CHDIT complex and fit of the band maxima to the Morse oscillator (eq 6), the assignments of the overtone transitions can be made:

$$\frac{\tilde{\nu}}{\nu} = \tilde{\omega} - (\mathrm{v} + 1)\tilde{\omega}x \qquad (6)$$

At the first overtone region ($\Delta v = 2$), the CHDIT bands at 5610 and 5720 cm^{-1} can be attributed to the $|2\rangle|0\rangle$ and $|0\rangle|2\rangle$ pure LM states of CH_{m1} and CH_{m2}, respectively (Table 5 and Figure 1). The band at 5797 cm^{-1} can be assigned to the $|1\rangle|1\rangle$ LM combination state of CH_2 group. Two intense peaks at 5915 and 6001 cm^{-1} belong to two different CH olefinic bonds of CHDIT: terminal and nonterminal. Two other bands appearing at 5661 and 5828 cm^{-1} can be tentatively assigned to local mode−normal mode (LM−NM) combinations, indicating significant coupling of the CH stretch to the other modes in this region. The assignments for the gas-phase data are similar to these of the liquid-phase spectra (Table 6). Because bands are narrower in gas-phase spectra, an additional combination band at 5981 cm^{-1} can be seen between two olefinic peaks (Figure 4). The total aliphatic to olefinic relative intensities obtained from the peak fitting routine are (1.0):(**1.2**/1.1) for the liquid phase and (1.0):(1.3) for the gas-phase data, which are not in good agreement with the calculated value (Table 8). Only pure LM transitions and LM combinations have been used in relative intensity estimations. The agreement improves with the inclusion of the LM−NM combinations yielding (1.0):(**1.1**/0.8) and (1.0):(0.9) relative intensity for the liquid and gas phases, respectively.

TABLE 2: Calculated, Scaled, and Experimental Local Mode Parameters for the CH Bonds of 1,3-CHD

	$\tilde{\omega}_{exp}$		$\tilde{\omega}x_{exp}$		$\tilde{\omega}_{calc}{}^{c}$ (scaled)			$\tilde{\omega}x_{calc}{}^{c}$ (scaled)		
bond	liq[a]	vap[b]	liq[a]	vap[b]	calc	liq	vap	calc	liq	vap
CH_{ax}	3014 ± 6	2997 ± 2	76.5 ± 1.4	70.2 ± 0.4	3144	2971	2994	66.0	62.2	63.3
CH_{eq}	3050 ± 6	3074 ± 17	63.5 ± 1.4	64.9 ± 3.2	3208	3031	3055	64.8	61.0	62.1
CH_{ol}	3128 ± 7	3155 ± 1	56.0 ± 1.7	58.9 ± 0.1	3315	3132	3145	62.9	58.2	59.2
$CH_{ol'}$	3128 ± 7	3155 ± 1	56.0 ± 1.7	58.9 ± 0.1	3323	3139	3153	62.6	58.0	58.9

[a] Data from the first, second, and third overtone regions have been used to determine the experimental LM parameters for the liquid phase. [b] Taken from ref 20. [c] Calculated with the HF/6-311+G(d,p) method.

TABLE 3: Calculated, Scaled, and Experimental Local Mode Parameters for the CH Bonds of CHDIT

	$\tilde{\omega}_{exp}$		$\tilde{\omega}x_{exp}$		$\tilde{\omega}_{calc}{}^{b}$ (scaled)			$\tilde{\omega}x_{calc}{}^{b}$ (scaled)		
bond	liq[a]	vap	liq[a]	vap	calc	liq	vap	calc	liq	vap
CH_{m1}	3006 ± 11		66.5 ± 2.3		3126	2954	2977	68.3	64.3	65.5
CH_{m2}	3065 ± 7		68.0 ± 1.7		3157	2983	3006	67.3	63.4	64.5
CH_{ol_t}	3170 ± 31		72.0 ± 7.5		3211	3033	3047	66.4	61.5	62.5
$CH_{ol_{nt}}$	3206 ± 5		68.0 ± 1.2		3288	3106	3120	64.0	59.3	60.2

[a] Data from the first, second and third overtone regions have been used to determine the experimental LM parameters for the liquid phase. [b] Calculated with the HF/6-311+G(d,p) method.

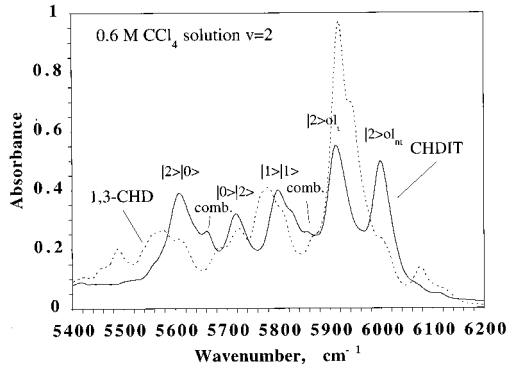

Figure 1. First vibrational overtone spectra of CHDIT (solid line) and 1,3-CHD (dashed line) recorded for the 0.6 M CCl_4 solution at room temperature in a 1 cm path length quartz cell. The CHDIT transitions are labeled according to assignments reported in Table 5.

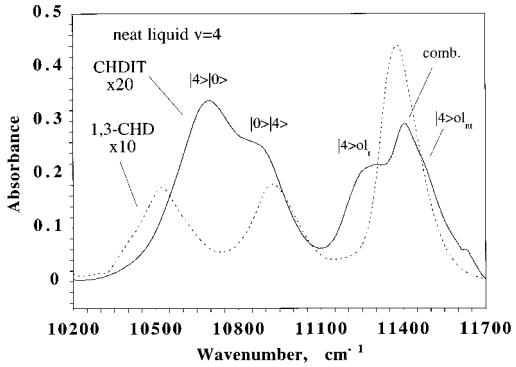

Figure 3. Third vibrational overtone spectra of CHDIT (solid line) and 1,3-CHD (dashed line) recorded for the neat liquid samples at room temperature in a 1 cm path length quartz cell. The CHDIT transitions are labeled according to assignments reported in Table 5.

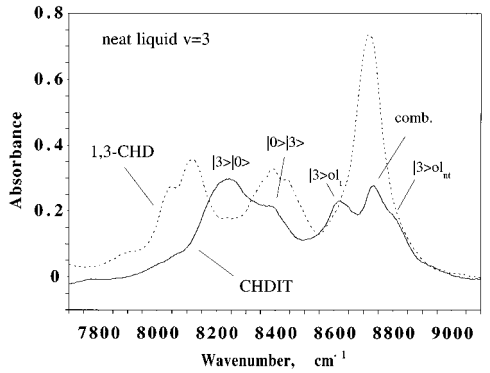

Figure 2. Second vibrational overtone spectra of CHDIT (solid line) and 1,3-CHD (dashed line) recorded for the neat liquid samples at room temperature in a 1 cm path length quartz cell. The CHDIT transitions are labeled according to assignments reported in Table 5.

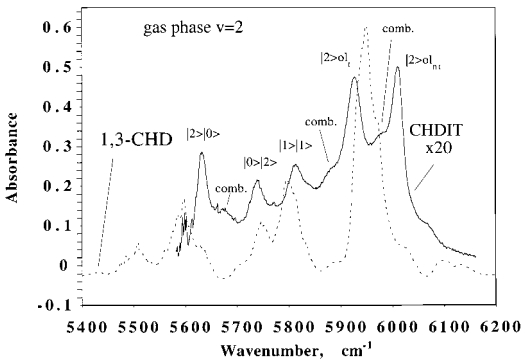

Figure 4. First vibrational overtone spectra of CHDIT and 1,3-CHD recorded for the gas-phase samples. Ligand spectrum was recorded at room temperature with sample pressure of 60 Torr. CHDIT spectrum was recorded at 100 °C with estimated sample pressure of 0.5 Torr. The path length is 3 m for both the ligand and the complex. The CHDIT transitions are labeled according to assignments reported in Table 6.

The calculated intensity of aliphatic CHs of CHDIT is much higher than experimentally observed.

At the second overtone ($\Delta v = 3$), two main absorption features with substructure are observed for both CCl_4 solution and neat liquid spectra (Figure 2) of CHDIT. The similarity between these two sets of data suggests that the solvent does not interact with the CHDIT and both the first overtone solution and the second and third overtone neat liquid spectra can be combined in the analysis. The deconvolution of this spectrum yields five bands located at 8229, 8385, 8618, 8733, and 8805 cm^{-1}. The intense peak at 8229 cm^{-1} is assigned to the $|3\rangle|0\rangle$ state of CH_{m1}, and the partially resolved transition at 8385 cm^{-1} belongs to the $|0\rangle|3\rangle$ state of CH_{m2} . The band assigned to $|3\rangle_{ol_t}$ is located at 8618 cm^{-1}, and the $|3\rangle_{ol_t}$ transition appears as a high-energy shoulder of the 8733 cm^{-1} band and has an energy of 8805 cm^{-1}. The intense 8733 cm^{-1} peak can be attributed to the LM−NM combination initiated by the metal complexation. The LM−NM combination band observed at this overtone is absent in the uncomplexed 1,3-CHD spectrum. The experimental

TABLE 4: Observed and Calculated Frequencies, Intensities, and Assignments for CH Stretching Vibrational Spectra of CCl_4 Solution and Neat Liquid 1,3-CHD

	observed[b]		calculated[c]	
state[a]	$\tilde{\nu}$, cm^{-1}	f	$\tilde{\nu}$, cm^{-1}	f
comb.	5489	2.4×10^{-8}		
$\|2\rangle\|0\rangle$	5569	1.3×10^{-7}	5567	8.3×10^{-8}
$\|0\rangle\|2\rangle$	5720	4.0×10^{-8}	5713	1.4×10^{-7}
$\|1\rangle\|1\rangle$	5776	1.4×10^{-7}	5792	2.2×10^{-7}
comb.	5808	4.6×10^{-8}		
$\|2\rangle_{ol+ol'}$	5917	3.8×10^{-7}	5920	3.8×10^{-7}
comb.	6077	1.8×10^{-8}		
comb.	**8032** (8031)	**3.7** $\times$ **10**$^{-9}$ (2.4×10^{-9})		
$\|3\rangle\|0\rangle$	**8119** (8116)	**1.9** $\times$ **10**$^{-8}$ (4.6×10^{-8})	8122	2.7×10^{-8}
$\|0\rangle\|3\rangle$	**8381** (8383)	**2.3** $\times$ **10**$^{-8}$ (3.4×10^{-8})	8384	2.6×10^{-8}
$\|2\rangle\|1\rangle$	**8456** (8459)	**3.0** $\times$ **10**$^{-8}$ (8.4×10^{-9})	8485	3.0×10^{-9}
$\|1\rangle\|2\rangle$			8592	2.0×10^{-9}
$\|3\rangle_{ol+ol'}$	**8718** (8724)	**3.9** $\times$ **10**$^{-8}$ (6.9×10^{-8})	8712	4.0×10^{-8}
$\|4\rangle\|0\rangle$	10 528	1.3×10^{-9}	10 524	3.3×10^{-9}
$\|0\rangle\|4\rangle$	10 931	1.4×10^{-9}	10 927	2.4×10^{-9}
$\|4\rangle_{ol+ol'}$	11 386	2.4×10^{-9}	11 392	4.1×10^{-9}

[a] First quantum number refers to CH_{ax}, second quantum number refers to CH_{eq}. [b] Numbers in parentheses are 0.6 M CCl_4 solution data; boldface numbers represent neat liquid 1,3-CHD. [c] Calculated with the experimental LM parameters from Table 2 and HF/6-311+G(d,p) dipole moment function.

TABLE 5: Observed and Calculated Frequencies, Intensities, and Assignments for CH Stretching Vibrational Spectra of CCl_4 Solution and Neat Liquid CHDIT

	observed[b]		calculated[c]	
state[a]	$\tilde{\nu}$, cm^{-1}	f	$\tilde{\nu}$, cm^{-1}	f
$\|2\rangle\|0\rangle$	**5611** (5610)	**1.0** $\times$ **10**$^{-7}$ (1.4×10^{-7})	5612	2.7×10^{-7}
comb.	**5662** (5661)	**1.7** $\times$ **10**$^{-8}$ (2.5×10^{-8})		
$\|0\rangle\|2\rangle$	**5718** (5720)	**6.0** $\times$ **10**$^{-8}$ (7.9×10^{-8})	5721	1.6×10^{-7}
$\|1\rangle\|1\rangle$	**5803** (5797)	**9.3** $\times$ **10**$^{-8}$ (6.6×10^{-8})	5804	2.7×10^{-7}
comb.	**5848** (5828)	**1.3** $\times$ **10**$^{-8}$ (8.8×10^{-8})		
$\|2\rangle_{ol_t}$	**5914** (5915)	**1.6** $\times$ **10**$^{-7}$ (1.8×10^{-7})	5908	2.0×10^{-7}
$\|2\rangle_{ol_{nt}}$	**6001** (6001)	**1.4** $\times$ **10**$^{-7}$ (1.4×10^{-7})	6004	1.8×10^{-7}
$\|3\rangle\|0\rangle$	**8229** (8231)	**4.0** $\times$ **10**$^{-8}$ (4.9×10^{-8})	8220	4.9×10^{-8}
$\|0\rangle\|3\rangle$	**8385** (8394)	**1.5** $\times$ **10**$^{-8}$ (1.6×10^{-8})	8378	3.3×10^{-8}
$\|3\rangle_{ol_t}$	**8618** (8619)	**1.7** $\times$ **10**$^{-8}$ (1.8×10^{-8})	8646	2.2×10^{-8}
comb.	**8733** (8732)	**1.1** $\times$ **10**$^{-8}$ (1.5×10^{-8})		
$\|3\rangle_{ol_{nt}}$	**8805** (8800)	**1.0** $\times$ **10**$^{-8}$ (1.0×10^{-8})	8802	2.5×10^{-8}
$\|4\rangle\|0\rangle$	10 686	1.7×10^{-9}	10 694	4.8×10^{-9}
$\|0\rangle\|4\rangle$	10 897	1.2×10^{-9}	10 899	2.7×10^{-9}
$\|4\rangle_{ol_t}$	11 257	0.7×10^{-9}	11 240	2.5×10^{-9}
comb.	11 404	0.6×10^{-9}		
$\|4\rangle_{ol_{nt}}$	11 459	0.8×10^{-9}	11 464	2.1×10^{-9}

[a] First quantum number refers to CH_{m1}; second quantum number refers to CH_{m2}. [b] Numbers in parentheses are 0.6 M CCl_4 solution data; boldface numbers represent neat liquid CHDIT. [c] Calculated with the experimental LM parameters from Table 3 and HF/6-311+G(d,p) dipole moment function.

TABLE 6: Observed Frequencies, Intensities, and Assignments for the CH Stretching Vibrational Spectrum of Gaseous CHDIT at the First Overtone Region

state[a]	$\tilde{\nu}$, cm^{-1}	f
$\|2\rangle\|0\rangle$	5635	1.2×10^{-7}
comb.	5678	6.8×10^{-8}
$\|0\rangle\|2\rangle$	5740	8.8×10^{-8}
$\|1\rangle\|1\rangle$	5815	1.2×10^{-7}
comb.	5877	9.0×10^{-8}
$\|2\rangle_{ol_t}$	5928	2.4×10^{-7}
comb.	5981	1.3×10^{-7}
$\|2\rangle_{ol_{nt}}$	6014	1.8×10^{-7}

[a] First quantum number refers to CH_{m1}; second quantum number refers to CH_{m2}.

total aliphatic to total olefinic intensity ratio for this overtone is (1.0):(**0.5**/0.4), which is close to the calculated (1.0):(0.6) value.

The spectral pattern at the third overtone ($\Delta v = 4$) is similar to that of the second overtone spectrum (Figure 3). Five transitions located at 10 686, 10 897, 11 257, 11 404, and 11 459 cm^{-1} can be assigned to the $|4\rangle|0\rangle$ of CH_{m1}, $|0\rangle|4\rangle$ of CH_{m2}, $|4\rangle_{ol_t}$, LM−NM combination, and $|4\rangle_{ol_{nt}}$, respectively. The experimental aliphatic to olefinic intensity ratio for the third

TABLE 7: Calculated CH and Olefinic CC Bond Lengths[a] in 1,3-CHD and CHDIT

bond	HF/3-21G(*)	HF/6-311+G(d,p)	pBP/DN**
	1,3-Cyclohexadiene		
CH_{ax}	1.089	1.091	1.117
CH_{eq}	1.083	1.086	1.108
CH_{ol}	1.073	1.077	1.099
CH_{ol}	1.073	1.076	1.099
C_1C_2; C_3C_4	1.322	1.325	1.354
C_2C_3	1.476	1.475	1.465
	Cyclohexadiene Iron Tricarbonyl		
CH_{m1}	1.087	1.091	1.112
CH_{m2}	1.086	1.089	1.107
CH_{ol_t}	1.080	1.084	1.101
$CH_{ol_{nt}}$	1.074	1.079	1.098
C_1C_2; C_3C_4	1.472	1.461	1.435
C_2C_3	1.372	1.374	1.424

[a] Bond lengths are given in angstroms.

TABLE 8: Total Relative CH Olefinic to CH Methylenic Intensities for 1,3-CHD and CHDIT

	1,3-CHD		CHDIT	
υ	obs[a]	calc[b]	obs[a]	calc[b]
2 (gas phase)	1.1	1.1	1.3	
2	1.1	0.9	**1.2** (1.1)	0.5
3	**0.9** (0.8)	0.7	**0.5** (0.4)	0.6
4	**0.9**	0.7	**0.5**	0.6

[a] Numbers in parentheses are 0.6 M CCl_4 solution data; boldface numbers represent neat liquid CHDIT. [b] Calculated with the experimental LM parameters from Tables 2 and 3 and HF/6-311+G(d,p) dipole moment function.

overtone is (1.0):(**0.5**), with the calculated number being (1.0):(0.6). For this overtone, the agreement between the experiment and calculations is good.

The total absolute intensities presented in Table 9 show good agreement between the experimental and calculated values for the first overtone. The agreement remains satisfactory for the higher overtones. Previous calculations[20] have shown that absolute intensities calculated with HF/6-311+(d,p) dipole moment functions result in calculated intensities that are larger than the experimental values and the discrepancy between the two increases upon going to the higher overtone. The difference between the experimental and calculated oscillator strengths is similar for 1,3-CHD and CHDIT. This suggests that the HF theory is describing the CHDIT transition metal complex relatively well.

C. Bonding in CHDIT. The relative shifts of the CH olefinic overtone transitions for CHDIT and 1,3-CHD can provide information about the structure and bonding in the complex. Upon complexation, the CH_{nt} olefinic bond in the complex becomes shorter than CH_{ol} of 1,3-CHD as indicated by, e.g., a 73 cm^{-1} blue shift at the third overtone. The 129 cm^{-1} red shift for CH_t relative to the CH_{ol} peak in the 1,3-CHD third overtone spectrum indicates the lengthening of this bond. The empirical relationship between the experimental frequency shift ($\Delta\tilde{\nu}$) and change in the bond length (Δr) for a particular overtone (υ) has been developed for halogenated benzenes[10] and later applied to estimate the bond length changes in butadiene iron tricarbonyl upon complexation.[18] This type of relationship was reported to be basis set-dependent.[42] To estimate the changes to the CH olefinic bond length upon complexation, a similar type of correlation (eq 7) was derived from a HF/6-311G** basis set CH olefinic bond lengths and experimental overtone data for 1,3-dienes and 1-alkenes:[43]

$$\Delta r = \frac{\Delta\tilde{\nu}}{13.2\upsilon}(0.001) \qquad (7)$$

On the basis of this relationship, it can be estimated that the CH_{nt} is 0.001 Å shorter and the CH_t is 0.002 Å longer in the complex than the olefinic CH bond in 1,3-CHD.

The experimental CH olefinic overtone transition energies reported in the literature for the gas phase at the third overtone lie in the range from 11 143 cm^{-1} for 2-methyl-2-butene[43] to 11 652 cm−1 for cyclopentadiene,[16] while the energy of the shortest CH methylenic transition, determined from the mechanical frequency and anharmonicity reported for cyclopentane,[44] is 11 256 cm^{-1}. On the basis of comparison between the liquid-phase (Table 4 in this work) and gas-phase (Table 1 in ref 20) overtone transition energies for 1,3-CHD, the liquid-phase transitions are expected to be red-shifted by about 55 cm^{-1} at this overtone relative to the gas-phase energies. The CH_t of liquid CHDIT absorbs at 11 257 cm^{-1}, making it either a short CH aliphatic or very long CH olefinic bond. The transition belonging to the CH_{nt} is located at 11 459 cm^{-1} and has a typical olefinic character. This, in turn, leads to the conclusion that the structure and bonding in the CHDIT complex is close to the situation represented by structure **4**. The overtone spectroscopy results clarify the microwave spectroscopy results by favoring structure **4** over structure **3**.

The qualitative changes in the CH methylenic bond length can be tracked down from the band shifts in the spectra. The separation between the CH methylenic transitions decreases in the spectrum of the complex, indicating that CH methylenic bonds are closer in length after complexation. The comparison between the overtone spectra of 1,3-CHD and CHDIT reveals that the lower energy CH methylenic band is 160 cm^{-1} blue-shifted at the third overtone region. The other transition is red-shifted by only 34 cm^{-1} at this region. These shifts indicate the significant shortening of one of the methylenic CH bonds (former CH_{ax} in 1,3-CHD) while the other CH barely changes its length.

The results for CHDIT can be compared to the previous observations for butadiene iron tricarbonyl (BDIT).[18] These two molecules contain similar π-systems that interact with the Fe(CO)$_3$ fragment. BDIT has one extra CH olefinic bond, which complicates the analysis of the overtone spectrum. In CHDIT, however, the presence of the rigid six-membered ring introduces steric strain effects, which compete with the complexation effects. The third overtone spectrum of BDIT indicated that nonterminal olefinic CHs become shorter upon complexation.[18] Among two terminal CH bonds (one cis and one trans to the middle CC bond of 1,3-butadiene), the terminal trans bond lengthens while the terminal cis bond does not change its length significantly. The situation is similar for the CHDIT, where the corresponding bonds show the same changes after complexation. This indicates that the olefinic π-systems in 1,3-butadiene and 1,3-CHD interact with iron tricarbonyl the same way and the cyclic geometry of the latter ligand has little effect on the complexation. The observed changes for the CH aliphatic bonds of 1,3-CHD during complexation can be explained by the change in the six-membered ring geometry. In the free ligand, the two double bonds do not lie in the same plane. The dihedral angle between them is about 15° [HF/6-311+G(d,p)], and CH

TABLE 9: Total Absolute Oscillator Strengths for CCl_4 Solution and Neat Liquid 1,3-CHD and CHDIT

	1,3-CHD		CHDIT	
υ	obs[a]	calc[b]	obs[a]	calc[b]
1		5.8×10^{-5}		14.3×10^{-5}
2	7.8×10^{-7}	8.2×10^{-7}	$\mathbf{5.8 \times 10^{-7}}$ (7.2×10^{-7})	10.9×10^{-7}
3	$\mathbf{11.5 \times 10^{-8}}$ (16.0×10^{-8})	9.8×10^{-8}	$\mathbf{9.3 \times 10^{-8}}$ (10.8×10^{-8})	12.6×10^{-8}
4	$\mathbf{5.1 \times 10^{-9}}$	9.4×10^{-9}	$\mathbf{5.0 \times 10^{-9}}$	12.2×10^{-9}
5		12.5×10^{-10}		13.3×10^{-10}

[a] Numbers in parentheses are 0.6 M CCl_4 solution data; boldface numbers represent neat liquid CHDIT. [b] Calculated with the HF/6-311+G(d,p) dipole moment functions and the experimental LM parameters.

methylenic bonds exhibit pseudoaxial and equatorial character. The complexation forces the two double bonds to become coplanar, thus introducing some steric strain in the ring and making CH methylenic bonds closer in character and length.

Conclusions

The CH stretching overtone spectra of liquid ($\Delta v = 2-4$) and gaseous ($\Delta v = 2$) cyclohexadiene iron tricarbonyl are recorded and compared to the corresponding spectra of uncomplexed 1,3-cyclohexadiene. The spectra have been assigned by use of HCAO local mode calculations and supported by the results of ab initio geometry optimization. The effect of complexation is to lengthen the CH terminal olefinic and shorten the CH nonterminal olefinic bonds. This results in appearance of two CH olefinic transitions in CHDIT spectrum, in contrast to the single olefinic peak observed for the uncomplexed ligand. The different methylenic bonds become similar in length, resulting in the appearance of two partially resolved CH methylenic peaks in the overtone spectrum of the complex. The experimental features obtained in this work support a structure of the complex where the central diene bond of the complexed ligand has a double-bond character while the terminal diene bonds are close to single CC bonds. Additional transitions absent in the spectrum of 1,3-cyclohexadiene are observed for the complex and are attributed to the local mode−normal mode combinations originating from the new channels for vibrational coupling created by the complexation.

Acknowledgment. We thank Bowling Green State University (A.V.F. and D.L.S.), University of Otago (H.G.K.), and Marsden Fund administered by the Royal Society of New Zealand (H.G.K.) for providing the financial support. A.V.F. is also thankful to the University of Manitoba for the Visiting Researcher appointment. K.M.G., B.B., and A.V.F. are grateful to the Natural Sciences and Engineering Research Council of Canada for financial support. We are grateful to Geoffrey R. Low for helpful discussions.

References and Notes

(1) Crabtree, R. H. *The Organometallic Chemistry of Transition Metals*; John Wiley and Sons: New York, 1988.
(2) Pruchnik, F. P.; Duraj, S. A. *Organometallic Chemistry of Transition Elements*; Plenum Press: New York, 1990.
(3) Karel, K. J.; Brookhart, M.; Aumann, R. *J. Am. Chem. Soc.* **1981**, *103*, 2695.
(4) Kruczynski, L.; Takats, J. *Inorg. Chem.* **1976**, *15*, 3140.
(5) Crews, P. *J. Am. Chem. Soc.* **1973**, *95*, 636.
(6) Ratnayake Bandara, B. M.; Birch, A. J.; Raverty, W. D. *J. Chem. Soc., Perkin Trans. 1* **1982**, 1745.
(7) Tam, W.; Eaton, D. F.; Calabrese, J. C.; Williams, I. D.; Wang, Y.; Andreson, A. G. *Chem. Mater.* **1989**, *1*, 128.
(8) Henderson, G. L.; Roehrig, M. A.; Wikrent, P.; Kukolich, S. G. *J. Phys. Chem.* **1992**, *96*, 8303.
(9) (a) Quack, M. *Annu. Rev. Phys. Chem.* **1990**, *41*, 839. (b) Henry, B. R. *Acc. Chem. Res.* **1987**, *20* (12), 429.
(10) Gough, K. M.; Henry, B. R. *J. Am. Chem. Soc.* **1984**, *106*, 2781.
(11) Gough, K. M.; Henry, B. R.; Schattka, B. J.; Wildman, T. A. *J. Phys. Chem.* **1991**, *95*, 1579.
(12) Snyder, R. G.; Aljibury, A. L.; Strauss, H. L.; Casal, H. L.; Gough, K. M.; Murphy, W. F. *J. Chem. Phys.* **1984**, *81*, 5352.
(13) Wong, J. S.; Moore, C. B. *J. Chem Phys.* **1982**, *77*, 603.
(14) Fedorov, A. V.; Snavely, D. L. *J. Phys. Chem. A* **1997**, *101*, 9042.
(15) Fedorov, A. V.; Snavely, D. L. *Chem. Phys.* **2000**, *254*, 169.
(16) VanMarter, T.; Olsen, C.; Snavely, D. *J. Phys. Chem.* **1994**, *98*, 5404.
(17) Fedorov, A. V.; Snavely, D. L. *J. Phys. Chem. A* **1999**, *103*, 7795.
(18) Fedorov, A. V.; Snavely, D. L. *J. Phys. Chem.* **1997**, *101*, 1451.
(19) Fedorov, A. V.; Snavely, D. L. *J. Phys. Chem. A* **1998**, *102* , 6234.
(20) Bellaiche-Sharpe, P.; Gough, K. M.; Schattka, B. J.; Low, G. R.; Kjaergaard, H. G. *J. Phys. Chem. A* **1998**, *102*, 10230.
(21) Albright, T. A.; Hoffman, R. *Chem. Ber.* **1978**, *111*, 1591.
(22) Burton, R.; Pratt, L.; Wilkinson, G. *J. Chem. Soc.* **1961**, 594.
(23) Butcher, S. S. *J. Chem. Phys.* **1965**, *42*, 1830.
(24) Fritz, H. P. *Chem. Ber.* **1959**, *92*, 780.
(25) Atkins, P. W. *Molecular Quantum Mechanics*, 2nd ed.; Oxford University Press: Oxford, U.K., 1983.
(26) Kjaergaard, H. G.; Proos, R. J.; Turnbull, D. M.; Henry, B. R. *J. Phys. Chem.* **1996**, *100*, 19273.
(27) Kjaergaard, H. G.; Yu, H.; Schattka, B. J.; Henry, B. R.; Tarr, A. W. *J. Chem. Phys.* **1990**, *93*, 6239.
(28) Kjaergaard, H. G.; Henry, B. R.; Tarr, A. W. *J. Chem. Phys.* **1991**, *94*, 5844.
(29) Kjaergaard, H. G.; Henry, B. R. *J. Chem. Phys.* **1992**, *96*, 4841.
(30) Kjaergaard, H. G.; Turnbull, D. M.; Henry, B. R. *J. Chem. Phys.* **1993**, *99*, 9438.
(31) Mortensen, O. S.; Henry, B. R.; Mohammadi, M. A. *J. Chem. Phys.* **1981**, *75*, 4800.
(32) SPARTAN, Version 5.0; Wavefunction Inc.: Irvine, CA, 1995.
(33) Frisch, M. J.; Trucks, G. W.; Schlegel, H. B.; Gill, P. M. W.; Johnson, B. G.; Robb, M. A.; Cheeseman, J. R.; Keith, T.; Petersson, G. A.; Montgomery, J. A.; Raghavachari, K.; Al-Laham, M. A.; Zakrzewski, V. G.; Ortiz, J. V.; Foresman, J. B.; Peng, C. Y.; Ayala, P. Y.; Chen, W.; Wong, M. W.; Andres, J. L.; Replogle, E. S.; Gomperts, R.; Martin, R. L.; Fox, D. J.; Binkley, J. S.; Defrees, D. J.; Baker, J.; Stewart, J. P.; Head-Gordon, M.; Gonzales, C.; Pople, J. A. *Gaussian 94*, revision D.4; Gaussian Inc.: Pittsburgh, PA, 1995.
(34) Kjaergaard, H. G.; Henry, B. R. *Mol. Phys.* **1994**, *83*, 1099.
(35) Kjaergaard, H. G.; Daub, C. D.; Henry, B. R. *Mol. Phys.* **1997**, *90*, 201.
(36) Kjaergaard, H. G.; Bezar, K. J.; Brooking, K. A. *Mol. Phys.* **1999**, *96*, 1125.
(37) Daub, C. D.; Henry, B. R.; Sage, M. L.; Kjaergaard, H. G. *Can. J. Chem.* **1999**, *77*, 1775.
(38) Low, G. R.; Kjaergaard, H. G. *J. Chem. Phys.* **1999**, *110*, 9104.
(39) Kjaergaard, H. G.; Henry, B. R. *J. Phys. Chem.* **1996**, *100*, 4749.
(40) Henry, B. R. *Vibr. Spectra Struct.* **1981**, *10*.
(41) Fang, H. L.; Swofford, R. L. *J. Chem. Phys.* **1980**, *73*, 2607.
(42) Gough, K. M.; Srivastava, H. K. *J. Phys. Chem.* **1996**, *100*, 5210.
(43) Fang, H. L.; Compton, D. A. C. *J. Phys. Chem.* **1988**, *92*, 7185.
(44) Wong, J. S.; MacPhail, R. A.; Moore, C. B.; Strauss, H. L. *J. Phys. Chem.* **1982**, *86*, 1478.